

# Stress Analysis of Non-persistent Rock Joints under Biaxial Loading

Omer S. Mughieda

**Abstract**—Two-dimensional finite element model was created in this work to investigate the stresses distribution within rock-like samples with offset open non-persistent joints under biaxial loading. The results of this study have explained the fracture mechanisms observed in tests on rock-like material with open non-persistent offset joints [1]. Finite element code SAP2000 was used to study the stresses distribution within the specimens. Four-nodded isoperimetric plain strain element with two degree of freedom per node, and the three-nodded constant strain triangular element with two degree of freedom per node were used in the present study. The results of the present study explained the formation of wing cracks at the tip of the joints for low confining stress as well as the formation of wing cracks at the middle of the joint for the higher confining stress. High shear stresses found in the numerical study at the tip of the joints explained the formation of secondary cracks at the tip of the joints in the experimental study. The study results coincide with the experimental observations which showed that for bridge inclination of  $0^\circ$ , the coalescence occurred due to shear failure and for bridge inclination of  $90^\circ$  the coalescence occurred due to tensile failure while for the other bridge inclinations coalescence occurred due to mixed tensile and shear failure.

**Keywords**—Finite element, open offset rock joint, SAP2000, biaxial loading

## I. INTRODUCTION

THE behavior of a rock mass is mainly controlled by the presence of the discontinuities within the rock. Rock masses are usually discontinuous in nature as a result of various geological processes. Consequently, joints and rock bridges form in the rock masses. Understanding of the initiation, propagation and coalescence of rock cracks is an important aspect in rock mechanics. Crack propagation and coalescence processes may contribute to rock failure in slopes, foundations and tunnels. Joint propagation and coalescence can reduce the stiffness of jointed rock masses causing the shear failure of rock slopes [2]. Also, joint propagation and coalescence can induce earthquakes by forming shear faults [3]. Only few studies have been performed on biaxial loading condition, some are presented by [4]. [4] performed uniaxial and biaxial loadings on jointed rock blocks and found three different failure modes under different joint geometry configurations: (a) tensile splitting through intact material; (b) shear and tensile failure or shear failure only on pre-existing joints; and (c) a mixed failure mechanism of the above two modes.

Omer S. Mughieda, is with Civil Engineering Department, Abu Dhabi University, Abu Dhabi, UAE, on leave from Jordan University of Science and Technology, Irbid, Jordan (phone:+971-50-1766847;e-mail: omer.mughieda@adu.ac.ae).

Also, concluded that orientation of joint sets and the level of intermediate principal stress play major roles with respect to the mode of failure. Many investigators have studied the crack propagation in different materials in uniaxial compression such as [5] and [6] on glass, [7] on plaster of Paris, [8], [9], [10], [11], [12], [13] on gypsum, [14] on rock like material mortar (Portland cement, sand and water), [15] on mortar (Portland cement, water and sand). Two types of crack patterns have been observed by those researchers: Wing cracks and secondary cracks. Wing cracks appear first; they are tensile cracks, which initiate at the tips of the joint (from now on the term joint will be used for preexisting cracks) and propagate steadily in a curvilinear path in the direction of the applied axial load. Reference [1] performed biaxial compression tests on block specimens made of rock like material (Portland cement: type I, water and sand) to study the effect of bridge inclination angle on the fracture mechanism of rock masses under biaxial loading condition. The present finite element work has been carried out to explain the results of the study by [1]. The present study focuses on investigation the stress distribution in the bridge area, which was the most important reason for the coalescence of fracture and eventually the failure of the specimens.

## II. EXPERIMENTAL WORKS

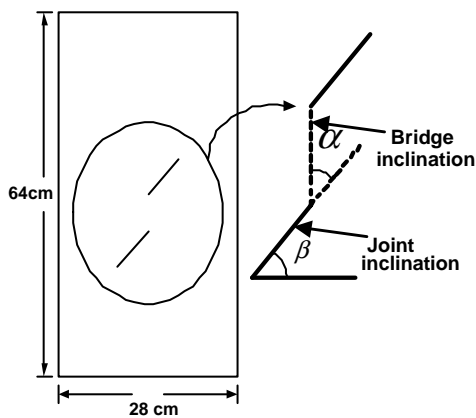
Reference [1] have performed a series of biaxial compression tests on blocks with offset non-persistent joints to study the effect of bridge inclination angle on the failure mechanism of blocks with open non persistent rock joints under biaxial loading. The inclination angle of the joints ( $\beta$ ) remained constant at  $45^\circ$  for all specimens and the inclination angle of the bridge ( $\alpha$ ) was changed from  $0^\circ$  to  $90^\circ$  with an increment of  $15^\circ$ . The specimens were tested under three different confining stresses: 0.35, 0.7 and 1.5 MPa. The lateral stress to unconfined compressive strength (11 MPa is an average value) ratios are: 0.032, 0.064 and 0.14, respectively. In all the tests, the confining load was applied first and held constant at the desired level, while the vertical load was increased until failure. The geometry of block tested and loading frame are shown in Figure 1.

## III. DESCRIPTION OF FINITE ELEMENT MODEL

In order to determine the state of stress before the wing crack initiation and coalescence, finite element analyses were performed on the crack arrangements that were studied experimentally. A linear elastic material was assumed for these analyses, mainly because there were no signs of major material damage prior to crack initiation and coalescence. Modulus of elasticity of approximately 10510 MPa was

obtained from the experimental load-displacement curves and used in the analyses. A Poisson's ratio of 0.25 was assumed.

Four-noded isoperimetric plain strain element with two degree of freedom per node, and the three-noded constant strain triangular element with two degree of freedom per node were used in the present study. The following boundary conditions were applied on the finite element model: zero vertical displacement along the bottom edge, and a uniform distribution load on the top surface, the magnitude of which was approximately the measured coalescence load (in MPa) for the crack geometry analyzed. It was assumed that the cracks were sufficiently far from the top and bottom of the block such that the exact distribution of loads on these edges did not significantly affect the stresses around the cracks. The three-dimensional effects in the experiments were neglected since the modeled used in the present study was two-dimensional.



a) Geometry of the specimens and pre-existing cracks

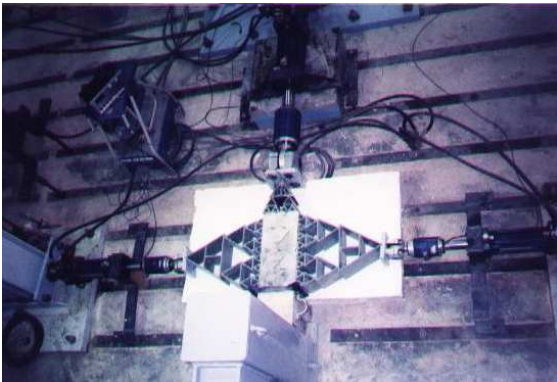


Fig. 1 a) Geometry of the specimens and pre-existing cracks, b) Loading frame. [1]

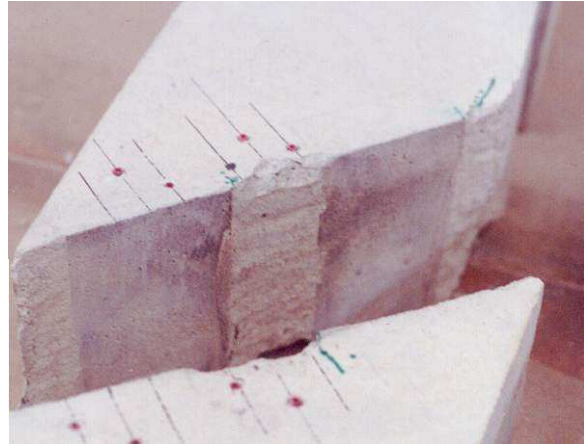
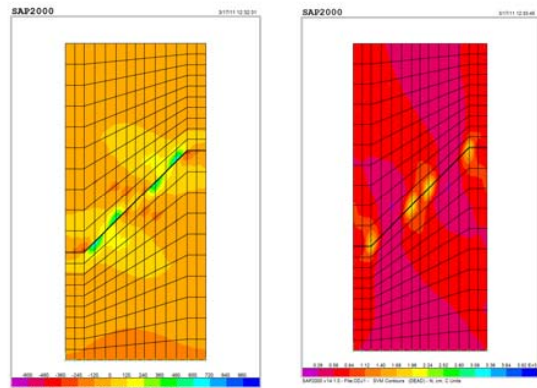


Fig. 2 Failure surface of ODJ1,  $\alpha = 0^\circ$ ,  $\beta = 45^\circ$  [1]

#### IV. LINEAR ELASTIC RESULTS AND DISCUSSION

##### A. Coplanar Joints ( $\beta = 45^\circ$ , $\alpha = 0^\circ$ )

The results of finite element are shown in Figures 3-5. As shown in these figures the shear strength is maximum in the region between the pre-existing cracks (bridge segment). Which implies that the shear stress was mainly responsible for the initiation and propagation of the secondary crack that caused the specimen failure. By investigating the plane of failure of the tested block in the experimental work a crushed material with many kink steps was observed, indicated that the shearing stress was responsible of block failure. This conclusion matches the results of finite element method.

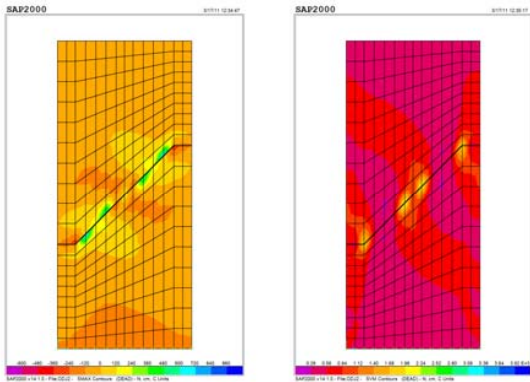


a) Maximum principal stresses b) Maximum shear stresses  
Fig. 3 a) Maximum principal stress and b) maximum shear stress around  $45^\circ$ - $0^\circ$  cracks. ( $\sigma_3 = 0.35\text{MPa}$ )

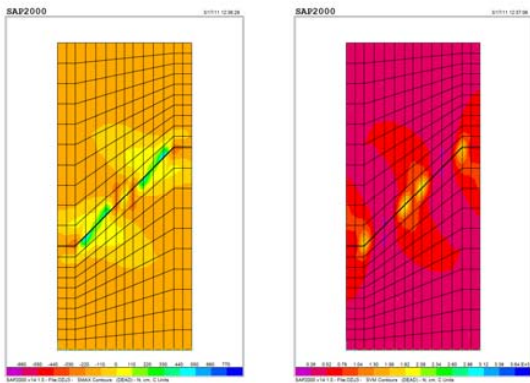
##### B. Slightly offset Joints ( $\beta = 45^\circ$ , $\alpha = 30^\circ$ )

Experimental work showed that shear and tensile stresses were both responsible for the crack initiation and propagation that caused failure of the sample. By investigating the results of finite elements method presented in Figures 6-8. The figures show that tensile stresses are concentrated at the tips of the joints, while shear stress values are high at the middle of the bridge segment, indicating shear failure. The effect of confining stress is also shown in these figures. As the

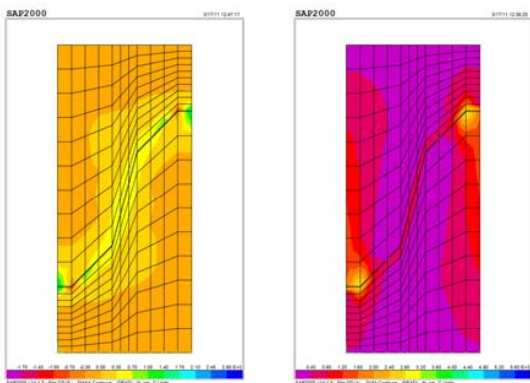
confining stress increases the principal stress increases in the bridge segment which resulted the suppressing of tensile failure and preventing the formation of wing crack.



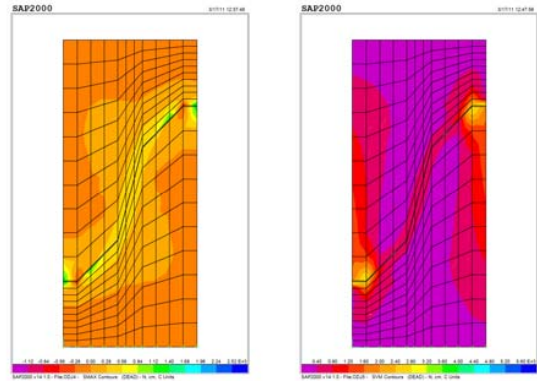
a) Maximum Principal Stresses      b) Maximum shear stresses  
Fig. 4 a) Maximum principal stress and b) maximum shear stress around 45°-0° cracks. ( $\sigma_3 = 0.7\text{MPa}$ )



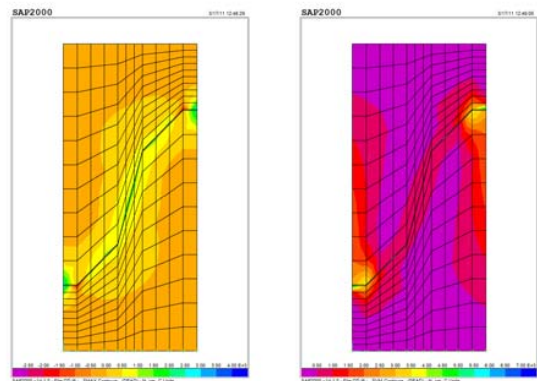
a) Maximum Principal Stresses      b) Maximum shear stresses  
Fig. 5 a) Maximum principal stress and b) maximum shear stress around 45°-0° cracks. ( $\sigma_3 = 1.5\text{MPa}$ )



a) Maximum Principal Stresses      b) Maximum shear stresses  
Fig. 6 a) Maximum principal stress and b) maximum shear stress around 45°-30° cracks, ( $\sigma_3 = 0.35\text{MPa}$ )



a) Maximum principal stresses      b) Maximum shear stresses  
Fig.7 a) Maximum shear stress and b) maximum principal stress around 45°-30° cracks, ( $\sigma_3 = 0.7\text{MPa}$ )



a) Maximum principal stresses      b) Maximum shear stresses  
Fig. 8 a) Maximum shear stress and b) maximum principal stress around 45°-30° cracks, ( $\sigma_3 = 1.5\text{MPa}$ )

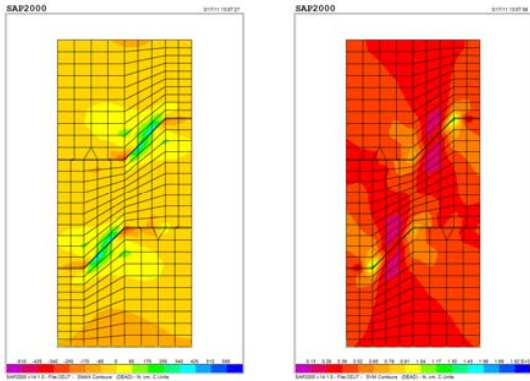
C. Offset joints ( $\beta = 45^\circ, \alpha = 45^\circ$ )

The experimental tests and finite elements analysis showed that wing cracks were formed due to high tensile stresses concentrated at the tips of the joints. These stresses caused the outer wing cracks to propagate and coalesce with the edge of the sample. While the shear stress concentration initiated a secondary crack at one of the inner tips. The characteristics of the failure surface indicated that high tensile stresses existed along the bridge. The final coalescence was caused by both tensile and shear stresses. Wing cracks were developed at the middle of the joint at low confining stress and disappeared at higher confining stress. Finite elements analysis results are shown in figures 9-11.

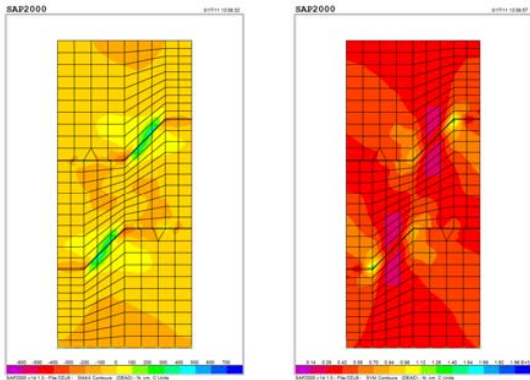
D. Sample with ( $\beta = 45^\circ, \alpha = 60^\circ$ )

Three specimens with  $\alpha = 60^\circ$  and  $\beta = 45^\circ$ , were tested under confining stresses of 0.35, 0.7 and 1.5 MPa, respectively. The experimental tests showed that, two wing cracks initiated at the outer and inner tips of the joints (pre-existing cracks). Then, a tensile crack initiated in the middle of the bridge segment. The surface of failure and the surface of wing cracks showed that, there is a pulverized or crushed material, and some traces of shear displacement could be seen in the vicinity

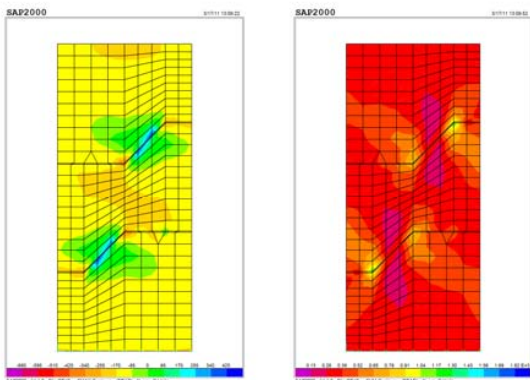
of the joint tip while a smooth surface without crushed material was noticed at the middle of the bridge segment Failure mode can be described as Type II (shear + tension). Finite element analysis results agree with the experimental tests results as shown in Figures 12-14.



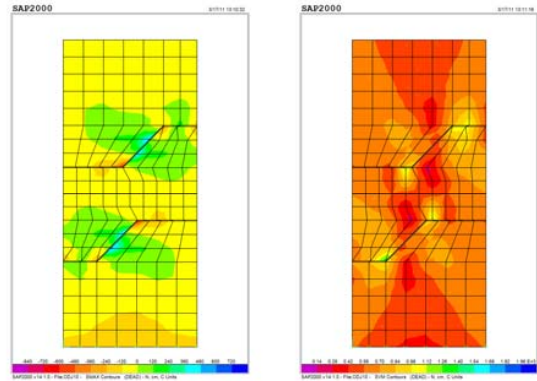
a) Maximum principal Stresses      b) Maximum shear stresses  
Fig. 9 a) Maximum shear stress and b) maximum principal stress around 45°-45° cracks, ( $\sigma_3=0.35\text{MPa}$ )



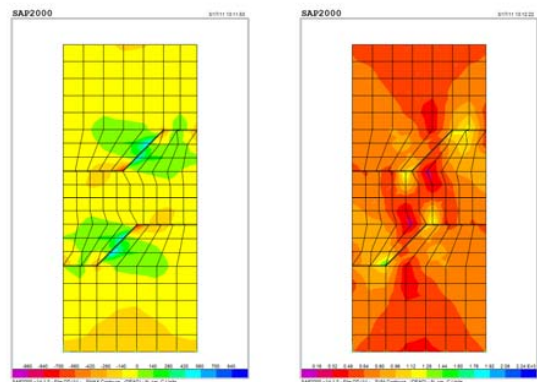
a) Maximum principal Stresses      b) Maximum shear stresses  
Fig. 10 a) Maximum shear stress and b) maximum principal stress around 45°-45° cracks, ( $\sigma_3=0.7\text{MPa}$ )



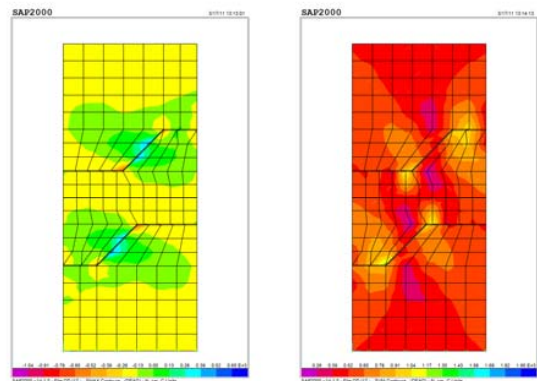
a) Maximum principal Stresses      b) Maximum shear stresses  
Fig. 11 a) Maximum shear stress and b) maximum principal stress around 45°-45° cracks, ( $\sigma_3=1.5\text{MPa}$ )



a) Maximum principal Stresses      b) Maximum shear stresses  
Fig. 12 a) Maximum shear stress and b) maximum principal stress around 45°-60° cracks, ( $\sigma_3=0.35\text{MPa}$ )



a) Maximum principal Stresses      b) Maximum shear stresses  
Fig. 13 a) Maximum shear stress and b) maximum principal stress around 45°-60° cracks, ( $\sigma_3=0.7\text{MPa}$ )

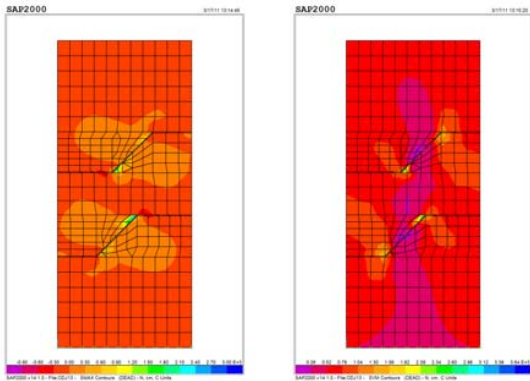


a) Maximum principal Stresses      b) Maximum shear stresses  
Fig. 14 a) Maximum shear stress and b) maximum principal stress around 45°-60° cracks, ( $\sigma_3=1.5\text{MPa}$ )

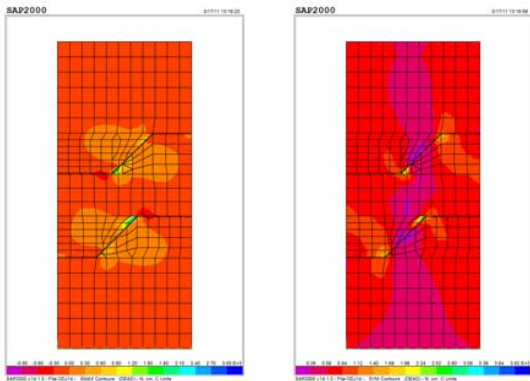
*E. Samples with ( $\beta=45, \alpha=75^\circ$ )*

Three specimens with  $\alpha=75^\circ$  and  $\beta=45^\circ$ , were tested under confining stresses of 0.35, 0.7 and 1.5 MPa, respectively. The experimental results showed that external wing cracks initiated and propagated steadily toward the vertical loading and in a

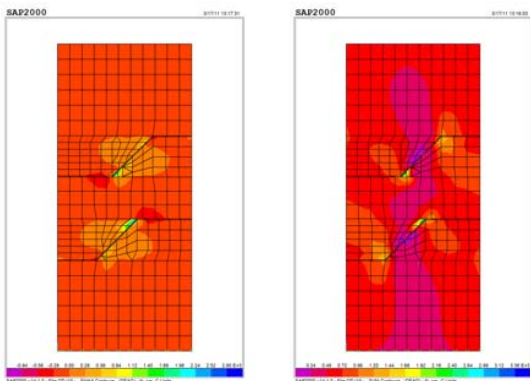
curvilinear path, and each inner wing crack initiated at the inner tip of each joint.



a) Maximum principal Stresses      b) Maximum shear stresses  
 Fig.15 a) Maximum shear stress and b) maximum principal stress around 45°-75° cracks, ( $\sigma_3=0.35\text{MPa}$ )



a) Maximum principal stresses      b) Maximum shear stresses  
 Fig. 16 a) Maximum shear stress and b) maximum principal stress around 45°-75° cracks



a) Maximum principal Stresses      b) Maximum shear stresses  
 Fig. 17 a) Maximum shear stress and b) maximum principal stress around 45°-75° cracks, ( $\sigma_3=1.5\text{MPa}$ )

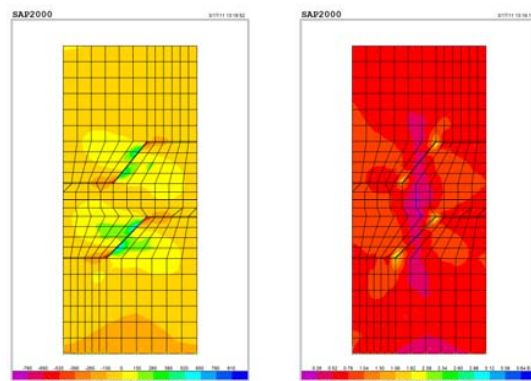
The failure was due to the coalescence of the shear cracks initiated at the inner tips of the joints and the tensile crack initiated in the rock bridge.

The surface of failure at the bridge area is tension-shearing surface. The finite elements results shown in Figures 15-17

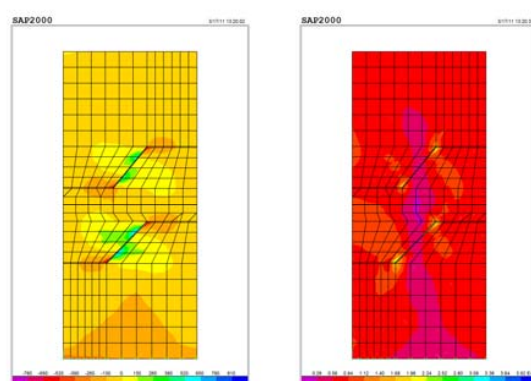
match the results of the experimental tests where tensile stress are concentrated in the region between the cracks, bridge segment, while shear stress values are high at the tip of the joints.

*F. Sample with ( $\beta=45, \alpha=90^\circ$ )*

Two specimens with  $\alpha = 90^\circ$  and  $\beta = 45^\circ$ , were tested under confining stresses of 0.35, 0.7 and 1.5 MPa, respectively. The experimental tests results showed that wing cracks at the out tips were initiated and propagated towards the applied load initially. Then, wing cracks initiated and propagated steadily at the middle of the joints. A tensile crack initiated at the middle of the bridge segment and propagated towards the tips of the pre-existing joints which eventually caused the specimen failure. The cracks that caused failure were created by tension. Same conclusion is reached by looking at the finite elements results, Figures 18-19. The tensile stress in the bridge segment area indicates that failure was mainly due to tension.



a) Maximum principal Stresses      b) Maximum shear stresses  
 Fig. 18 a) Maximum shear stress and b) maximum principal stress around 45°-90° cracks, ( $\sigma_3=0.35\text{MPa}$ )



a) Maximum principal Stresses      b) Maximum shear stresses  
 Fig. 19 a) Maximum shear stress and b) maximum principal stress around 45°-90° cracks, ( $\sigma_3=0.7\text{MPa}$ )

V.CONCLUSIONS

The failure of rock mass containing non-persistent joints is complicated and not well understood yet. Finite element analysis was performed to study the stresses condition at the

tips of the pre-existing joints and in the rock bridge segments on crack arrangements that were studied experimentally under biaxial loading condition. The bridge inclination was the main variable that controlled the mode of failure. For bridge inclination of  $0^\circ$ , the coalescence occurred due to shear failure and for bridge inclination of  $90^\circ$  the coalescence occurred due to tensile failure while for the other bridge inclinations coalescence occurred due to mixed tensile and shear failure. The effect of confining stress on mode of failure was insignificant. Finite element analyses based on two-dimensional finite element model and linear elastic material showed that tensile stress was mainly responsible for wing crack initiation while the shear stress was responsible for the secondary crack initiation.

## REFERENCES

- [1] Mughieda, O. S. and Karasneh, I (2006) Coalescence of offset rock joints under biaxial loading, *Geotechnical and Geological Engineering*, Vol. 24, No.4.
- [2] Einstein, H. H., Veneziano, D., Baecher, G. B. and O'Reilly, K. J. (1983) The effect of discontinuity persistence on rock stability, *International Journal of Rock Mechanics and Mining Sciences*, Geomechanical Abstracts, 20, 227–237.
- [3] Deng, Q. and Zhang, P. (1984) Research on the geometry of shear fracture zones, *Journal of Geophysical Research*, 89, 5669–5710.
- [4] Kulatilake, P. H., Park, J., and Malama, B. (2006) A new rock mass failure criterion for biaxial loading conditions. *Geotechnical and Geological Engineering*. Vol. 24: 871-888.
- [5] Hoek, E. and Bieniawski, Z. T. (1984) Brittle fracture propagation in rock under compression, *International Journal of Fracture*, 26, 276–294.
- [6] Brace, W. and Byerlee, J. (1967) Recent experimental studies of brittle fracture rocks, failure and breakage of rock, *AIME*, 57–81.
- [7] Lajtai, E. (1974) Brittle fracture in compression, *International Journal of Fracture*, 10(4), 525–339 536.
- [8] Horii, H. and Nemat-Nasser, S. (1986) Brittle failure in compression: splitting, faulting and brittle-ductile transition, *Philosophical Transaction of the Royal Society of London*, (1549), 337–374.
- [9] Pollard, D. D. and Aydin, A. (1988) Progress in understanding jointing over the past century, *Geological Society of America Bulletin*, 100. 2
- [10] Reyes, O. and Einstein, H. H. (1990) Stochastic and centrifuge modeling of jointed rock, Part I-Fracturing of jointed rock, Final Report submitted to the Air Force Office of Scientific Research and Air Force Engineering Services Center, U.S.A.
- [11] Germanovich, L. N, Ring, L. M, Carter, B. J, Ingraffea A. R, Dyskin A. V and Ustinov, K. B. (1995) Simulation of crack growth and interaction in compression. Proceedings of the 8<sup>th</sup> Int. Congs. on rock mechanics, Vol. 1, ISRM, Tokyo.
- [12] Shen, B., Stephanson, O., Einstein, H. H. and Ghahreman, B. (1995) Coalescence of fractures under shear stresses in experiments, *Journal of Geophysical Research*, 100(B4), 5975–5990.
- [13] Bobet, A. and Einstein, H. H. (1998) Fracture coalescence in rock-type materials under uniaxial and biaxial compression, *International Journal of Rock Mechanics and Mining Sciences*, 35(7), 863–888.
- [14] Mughieda, O. S. (1997) Failure mechanisms and strength of non-persistent rock joints, Ph.D. Thesis, University of Illinois at Urbana-Champaign, IL, U.S.A.
- [15] Mughieda, O., Alzo'ubi, A., 2004. Fracture mechanisms of offset rock joints- A laboratory investigations. *Geotechnical and Geological Engineering Journal*, Vol.22, 545-562, 2004.
- [16] Wilson, E. L., and Habibullah, A. (1989). *SAP90 users manual*, Computers and Structures Inc